JOURNAL OF SPACECRAFT AND ROCKETS
Vol. 34, No. 1, January–February 1997

Nonlinear Aeroprediction Methodology for Roll Position of 45 Degrees

F. G. Moore* and R. M. McInville†
U.S. Naval Surface Warfare Center, Dahlgren, Virginia 22448-5000

The U.S. Naval Surface Warfare Center, Dahlgren Division, aeroprediction code has been extended to the roll position of 45 deg (or fins in cross or *x* orientation). New technology developed and discussed includes wing-body and body-wing interference factors for this roll orientation and to angles of attack of 90 deg; approximate methods to estimate wing-alone center of pressure shift at high angles of attack and 45 deg roll position; and fin choking at high Mach number. This new technology allows aerodynamics to be estimated with average accuracy levels of ± 10% on normal and axial force coefficients and ± 4% of body length on center of pressure. Exceptions to these accuracy levels are at subsonic Mach number and high angle of attack, where wind-tunnel sting interference effects are present, and at high Mach number and angle of attack, where internal shock interactions from a forward fin onto an aft-mounted fin are present. Results are presented for several wing-body and wing-body-tail configurations at various Mach numbers and angles of attack to support this average accuracy level conclusion.

Nomenclature

AR	= aspect ratio $= b^2/A_W$
A_{REF}	= reference area (maximum cross-sectional area of body, if a body is present, or planform area of wing, if wing alone), ft^2
A_W	= planform area of wing in crossflow plane, ft^2
a	= speed of sound, ft/s
b	= wing span (not including body), ft
C_A	= axial force coefficient
C_M	= pitching moment coefficient (based on reference area and body diameter, if body present, or mean aerodynamic chord, if wing alone)
C_N	= normal-force coefficient
C_{N_B}	= normal-force coefficient of body alone
$C_{N_{B(V)}}$	= negative afterbody normal-force coefficient due to canard or wing-shed vortices
$C_{N_{B(W)}}$, $C_{N_{B(T)}}$	= normal-force coefficient on body in presence of wing or tail
$C_{N_{T(V)}}$	= negative normal-force coefficient component on tail due to wing or canard-shed vortex
C_{N_W}	= normal-force coefficient of wing alone
$C_{N_{W(B)}}$	= normal-force coefficient of wing in presence of body
C_{N_α}	= normal-force coefficient derivative
$(C_{N_\alpha})_L$	= linear component of normal-force coefficient derivative
$(C_{N_\alpha})_{NL}$	= nonlinear component of normal-force coefficient derivative
C_1, C_2	= dimensionless empirical factors used in nonlinear model of $k_{W(B)}$ to approximate effects due to high angle of attack or control deflection
c_r	= root chord, ft
c_t	= tip chord, ft
d_{REF}	= reference body diameter, ft
$K_{B(W)}$, $K_{B(T)}$	= ratio of additional body normal-force coefficient in presence of wing or tail to that of wing or tail alone at $\delta = 0$ deg
$[K_{B(W)}]_{\text{MIN}}$	= minimum value of $K_{B(W)}$ as percent of slender-body theory value
K_{B_1}	= lowest value of $[K_{B(W)}]_{\text{MIN}}$ for $\Phi = 45$ deg
$K_{W(B)}$, $K_{T(B)}$	= ratio of normal-force coefficient of wing or tail in presence of body to that of wing or tail alone at $\delta = 0$ deg
$k_{B(W)}$, $k_{B(T)}$	= ratio of additional body normal-force coefficient due to presence of wing or tail at a control deflection to that of wing or tail alone at $\alpha = 0$ deg
$k_{W(B)}$, $k_{T(B)}$	= ratio of wing or tail normal-force coefficient in presence of body due to a control deflection to that of wing or tail alone at $\alpha = 0$ deg
ℓ_B	= length of body, caliber (cal) (one body diameter) or ft
ℓ_a	= afterbody length, cal or ft
M	= Mach number $= V/a$
r	= radius of body, ft
s	= wing or tail semispan plus body radius in wing-body lift methodology
V	= velocity, ft/s
X_{CP}	= center of pressure (in ft or cal from some reference point that can be specified) in x direction
α	= angle of attack, deg
α_W, α_T	= local angle of attack of wing or tail ($\alpha + \delta$, deg)
$\Delta C_{N_{B(W)}}$	= additional normal-force coefficient on body due to presence of wing
δ	= control deflection (deg), positive leading edge up
λ	= taper ratio of a lifting surface $= c_t/c_r$
Φ	= circumferential position around body where $\Phi = 0$ is leeward plane with fins in plus fin arrangement, deg
∞	= freestream conditions

Introduction and Background

MANY of the world's missiles fly in either the roll-stabilized position of $\Phi = 0$ deg (or plus fin orientation) or $\Phi = 45$ deg (or cross fin orientation). The $\Phi = 0$ deg plane generally gives slightly more normal force and a slightly more stable configuration in pitch at a given angle of attack (AOA) than does the missile rolled to $\Phi = 45$ deg (the physics of why this occurs is discussed in the "Analysis" section). On the other hand, a missile in the $\Phi = 45$ deg plane is in a roll-stable position, which means less energy is required to maintain a constant roll orientation. Also, all four fins can be deflected simultaneously, giving 30–50% more normal force

Received Feb. 7, 1996; revision received July 1, 1996; accepted for publication Oct. 5, 1996.

*Senior Aerodynamicist, Weapons Systems Department, Dahlgren Division. Associate Fellow AIAA.

†Aerospace Engineer, Aeromechanics Branch, Weapons Systems Department, Dahlgren Division.

from control deflection than only two fins deflected in the $\Phi = 0$ deg roll position.

The latest version (1995)[1] of the U.S. Naval Surface Warfare Center, Dahlgren Division, aeroprediction code, AP95, calculates aerodynamics only in the $\Phi = 0$ deg plane. As such, aerodynamics at $\Phi = 45$ deg roll must be obtained from another aerodynamics code[2,3] or estimated from the AP95 $\Phi = 0$ deg results. However, both Refs. 2 and 3 use the so-called equivalent AOA method,[2] whereas Ref. 1 computes all the aerodynamic components directly based on linearized theory approaches at low AOA and databases at high AOA. The latter approach allows good engineering estimates of aerodynamics to be made all the way to AOA of 90 deg, whereas the equivalent AOA method appears to give good accuracy up to 25–30 deg AOA. It is the intent of this paper to discuss the physical phenomena that occur at the $\Phi = 0$ and 45 deg roll orientations and to summarize a semiempirical mathematical model that allows the AP95 to be extended to the $\Phi = 45$ deg plane. Details of this work can be found in Ref. 4.

The AP95 is an approximate analytical aeroprediction code primarily designed to provide preliminary estimates of aerodynamics for use in particle ballistic models, trim aerodynamic models, or structures and heat-transfer models. Static aerodynamics are generally estimated with average accuracy levels of $\pm 10\%$ and center of pressure (COP) within $\pm 4\%$ of the body length. To obtain aerodynamics estimation accuracy levels generally desired for full six-degree-of-freedom simulations requires either a more accurate numerical code[5] or wind-tunnel data or both. As such, the AP95 does not attempt to compute out-of-the-pitch-plane aerodynamics or coupling effects between the pitch and yaw planes. On the other hand, if one is interested in the $\Phi = 45$ deg plane, and control deflections are symmetric with respect to the pitch plane, then the AP95 code can be modified to allow aerodynamics for the $\Phi = 45$ deg plane. These modifications are made in a process analogous to the nonlinear semiempirical methodology of Ref. 1.

The overall approach to modify the AP95 code for nonlinear aerodynamics in the $\Phi = 45$ deg plane thus is very similar to that for the $\Phi = 0$ deg plane.[1,6] Linearized theories or slender body theory (SBT) are used for low AOA estimates, and the databases of Refs. 7–10 are used to develop empirical or semiempirical corrections to account for the nonlinearities that occur in normal force and COP with increasing AOA.

Analysis

As indicated in the "Introduction," the goal is to develop a nonlinear semiempirical model for cruciform missiles for the $\Phi = 45$ deg plane. It is envisioned that this model will be analogous to the $\Phi = 0$ deg plane methods in AP95, except the normal force and pitching moments due to the wing alone and interference aerodynamics will have to be derived for the $\Phi = 45$ deg roll orientation.

Referring to the total normal-force coefficient equation for a wing-body-tail configuration as given by Ref. 10, we have

$$C_N = C_{N_B} + \left[\left(K_{W(B)} + K_{B(W)}\right)\alpha + \left(k_{W(B)} + k_{B(W)}\right)\delta_W\right]\left(C_{N_\alpha}\right)_W + \left[\left(K_{T(B)} + K_{B(T)}\right)\alpha + \left(k_{T(B)} + k_{B(T)}\right)\delta_T\right]\left(C_{N_\alpha}\right)_T + C_{N_{T(V)}} + C_{N_{B(V)}} \quad (1)$$

The $C_{N_{B(V)}}$ term of Eq. (1), which is the downwash normal force on the body due to the wing-shed vortices, is neglected. This is because it is inherently included in the wind-tunnel data bases, and it is believed the errors in trying to analytically estimate the term, subtract it out on one configuration, and then add it back in later on a different configuration, are as large or larger than the errors from incorporating it into the $K_{B(W)}$ term.

Equation (1) can also be rewritten as

$$C_N = C_{N_B} + C_{N_{W(B)}} + C_{N_{B(W)}} + C_{N_{T(B)}} + C_{N_{B(T)}} + C_{N_{T(V)}} \quad (2a)$$

where it is understood that $C_{N_{B(T)}}$ encompasses the $C_{N_{B(V)}}$ term. For ease of implementation into an existing code designed primarily for linear aerodynamics, most of the terms in Eq. (2a) are separated into a linear and nonlinear contribution due to α or δ. For example, the wing-body term is computed in the AP95 code as follows:

$$C_{N_{W(B)}} = \left[\left(C_{N_\alpha}\right)_L + \left(C_{N_\alpha}\right)_{NL}\right]_W \left\{\left[\left(K_{W(B)}\right)_{\text{SBT}} + \left(\Delta K_{W(B)}\right)_{NL}\right]\alpha + \left(C_1\left[k_{W(B)}\right]_{\text{SBT}} + C_2\right)\delta_W\right\}(A_W/A_{\text{REF}}) \quad (2b)$$

The linear or small AOA terms of Eq. (2b) are estimated by linear theory (LT) or SBT. This gives the aeroprediction code a good fundamental basis for its aerodynamic estimates. The nonlinear corrections due to higher AOA or control deflection are estimated directly from component wind-tunnel databases.[7–10] Each of the other terms in Eq. (2a) is treated in a similar fashion to Eq. (2b) in the actual implementation into the aeroprediction code.

In the context of Eq. (2), we therefore seek the nonlinear definition of each of the terms in Eq. (2) for $\Phi = 45$ deg roll. It is expected that the body-alone term [first term of Eq. (2a)] will be independent of Φ. In reality, this is not necessarily the case for $M < 2$ and high AOA because of the asymmetric shedding of vortices. The mechanism of this shedding is not clear, but it is suspected that slight imperfections in the flow or body shape, from uniform or axisymmetric, respectively, could contribute to this phenomenon. At present, the aeroprediction code does not account for out-of-plane aerodynamics, and therefore the side force created by the asymmetric shedding of body vortices is not predicted. Also, in the Ref. 9 data, normal force varied by about 10% as a function of roll in the region of asymmetric vortex shedding. Instead of including this variation, it was averaged out.

Each of the remaining terms in Eq. (2) is predicted in a fashion analogous to the AP95 developed for $\Phi = 0$ deg, except here the quantities are for $\Phi = 45$ deg. As already mentioned, that approach was based on LT or SBT for small values of α and empirical databases[7–10] to develop nonlinear corrections for large α. As such, it is instructive to examine the fundamental impact of roll orientation on LT and SBT before proceeding to the nonlinear corrections, which are empirical in nature.

SBT and LT Results for Roll-Dependent Aerodynamics

References 11 and 12 were primary materials used for examining roll-dependence implications from slender-body and linearized theories. A somewhat detailed summary of these results is given for information purposes in Ref. 4. The summary of the key findings in Ref. 4, repeated here for convenience, are as follows.

1) For cruciform wings alone or a wing-body combination, the total normal force is independent of roll.

2) For a planar wing-body combination at roll, the loading on the windward plane panel is greater by an amount equal to that on the leeward plane panel. This means that if one is trying to design a code for lateral aerodynamics, roll dependence of each fin planform must be considered. On the other hand, if longitudinal aerodynamics are of primary interest, the total normal force on the entire wing planform can be considered.

3) For a cruciform wing-body-tail configuration at roll, eight vortices (four from wings and four image) are shed in the wing-body region, which adversely affects the tail lift. This is as opposed to four vortices (two from wings and two image) at $\Phi = 0$ deg.

4) The planar theory developed for wing-tail interference can be used to approximate the loss of lift on the tails at $\Phi = 45$ deg.

5) The aerodynamics of a cruciform wing-body-tail combination with zero control deflections are independent of roll position.

These findings for roll dependence from LT or SBT are quite useful in helping plan how to develop a nonlinear aeroprediction code for $\Phi = 45$ deg. Although the conclusions of LT roll dependence may not translate to the nonlinear case, we still use the findings to help guide the nonlinear code development. In particular, the item 1 conclusion implies use of the $\Phi = 0$ deg, wing-alone data for $\Phi = 45$ deg. This is quite important because the available wing-alone databases are all at $\Phi = 0$ deg. This means that any nonlinear wing-alone roll dependence is included in the interference factors rather than the wing-alone solution, which is independent of Φ.

The second major result of the key SBT/LT roll dependence findings is that, for cruciform missiles, we can use the same interference

approaches as in the AP95, except the constants need to be changed because of a different roll angle. The combination of these two conclusions is quite important because it basically allows direct usage of the AP95 code with different constants for the nonlinear interference terms at $\Phi = 45$ vs 0 deg.

The third significant conclusion is that for small AOA, wing-body-tail aerodynamics are independent of roll position. This allows the use of wing-tail interference methodology designed for planar computations for different roll orientations so long as the proper number of vortices is considered. Again, different nonlinear corrections are expected for the $\Phi = 45$ vs 0 deg roll position.

Nonlinear Aerodynamics Methods

This section describes the methods used for computing the nonlinear corrections for each of the terms in Eq. (2). These corrections, with the exception of the body alone, are all empirical in nature.

The wing- and body-alone methods for normal-force coefficient prediction are quite similar to those in Ref. 1. In Ref. 1, the wing-alone normal force was estimated by a fourth-order equation in AOA, with the constants chosen by the databases of Refs. 2, 7, and 8. The body-alone normal force was predicted by linearized theory combined with a modified version of the Allen Perkins viscous crossflow theory[13] at higher AOA.

The COP of the wing at $\Phi = 0$ deg roll was estimated by LT at low AOA and assuming the COP goes to the centroid of the presented area at AOA = 60 deg. The body-alone COP at $\Phi = 0$ deg was estimated by a weighted average of linearized theory and viscous crossflow theory with COP shifts based on data at transonic Mach numbers. The $\Phi = 45$ deg body-alone COP is assumed to be the same as that at $\Phi = 0$ deg.

A shift in the wing-body COP at $\Phi = 45$ deg has been derived.[4] This shift is driven by the asymmetric loading that occurs on the windward to leeward plane fins as AOA is increased.

To visualize this effect, imagine a missile rolled to $\Phi = 45$ deg and increasing in AOA. As AOA increases, two things occur. First, the windward plane fins carry more and more of the load compared to the leeward plane fins. Second, the local Mach number in the windward plane is different and typically lower than the leeward plane. This has the effect of shifting the wing-alone COP forward in the windward plane. Because the load and wing COPs are different on the windward and leeward plane fins, this results in a net forward shift in the COP for a $\Phi = 45$ deg roll compared to the $\Phi = 0$ deg computation of Ref. 1. This shift appears to occur for all Mach numbers, is largest at moderate AOA, and goes to zero at AOA of 0 and 90 deg. At 90 deg, the windward plane fins carry almost all the load compared to the leeward plane fins, but geometrically the fins are all aligned perpendicular to the AOA plane.

Mathematically, this geometrical shift can be approximated by[4]

$$(\Delta X_{CP})_{WB} = -\left[r + \left(\frac{b}{c_r + c_t}\right)\left(\frac{c_r}{2} - \frac{c_t}{3}\right)\right] \times \cos(\Phi)\sin(2\alpha)\left(\frac{0.8\alpha}{65}\right) \qquad \alpha \le 65\ \text{deg} \tag{3a}$$

$$= -0.8\left[r + \left(\frac{b}{c_r + c_t}\right)\left(\frac{c_r}{2} - \frac{c_t}{3}\right)\right] \times \cos(\Phi)\sin(2\alpha) \qquad \alpha > 65\ \text{deg} \tag{3b}$$

Equation (3) is added to the COP prediction at $\Phi = 0$ deg (Ref. 1) for the roll orientation of 45 deg.

Wing-Body and Body-Wing Interference due to AOA

The wing-body and body-wing interference factors were computed by using a combination of the Ref. 9 database for $0.6 \le M_\infty \le 4.6$ and the Ref. 10 database at $M = 0.1$. Outside these Mach limits, extrapolations were made to allow the methodology to compute aerodynamics at all Mach numbers. These extrapolations were not as difficult as they may seem because normal forces and COP have basically leveled out at $M = 4.6$, and further increases in Mach number produce fairly small changes in these parameters.

The wing-body interference factor is defined as

$$K_{W(B)} = \frac{C_{N_{W(B)}}}{C_{N_W}} \tag{4}$$

Here, $C_{N_{W(B)}}$ was measured directly in the database of Ref. 9 by having the wing in close proximity to the body and measuring directly the load on the wing in the presence of the body. Because the normal force was measured normal to a single fin, to get the normal force on the wing in the presence of the body at $\Phi = 45$ deg from the data required the data to be multiplied by cos Φ. To reduce measurement errors, the data from all four fins were averaged. No attempt was made to correct for wind-tunnel errors near zero AOA caused by flow misalignments. These errors can cause the normal-force curve to be shifted as much as a degree. This means that the $C_{N_{W(B)}}$ accuracy could have some slight errors near zero AOA.

On the basis of the accuracy analysis of Ref. 1, fairly accurate values of $K_{W(B)}$ can be expected for all but the highest aspect ratio where the wing planform area was only about 2% of the body planform area in the crossflow plane. C_{N_W} of Eq. (4) was arrived at from Ref. 1, which in turn used the databases of Refs. 2, 7, and 8.

The body-wing interference factor is defined as

$$K_{B(W)} = \frac{C_{N_{B(W)}}}{C_{N_W}} \tag{5}$$

Unfortunately, $C_{N_{B(W)}}$ was not a quantity that was measured directly in Ref. 7 but was computed from three other independent measurements of body alone, wing in conjunction with the body, and total normal force. The computation for $C_{N_{B(W)}}$ was then made by

$$C_{N_{B(W)}} = C_N - C_{N_B} - C_{N_{W(B)}} \tag{6}$$

As shown in the Ref. 1 error analysis, this process gave potential errors that were much higher than for $C_{N_{W(B)}}$, particularly for the smaller wings (AR $\ge$ 1.0) and higher Mach numbers ($M \ge 2.5$), where the $C_{N_{B(W)}}$ term decreased to the point where it was within the accuracy of the data. As a result, much more scatter in the data is expected for this term, and more engineering judgment is required in the empirical model development.

Unlike Ref. 9, Ref. 10 had a fairly large wing planform area compared to the body planform area (approximately 60%). Moreover, $C_{N_{B(W)}}$ was apparently measured separately. Hence, $C_{N_{B(W)}}$ could be computed based on direct measurements as well as calculated similar to Eq. (6). Also, data were obtained all the way to $\alpha = 90$ deg and at an r/s value of 0.25. As a result, more confidence is placed on the Ref. 10 body-wing interference at high AOA than the Ref. 9 data. Unfortunately, the Ref. 10 data were taken only at $M_\infty = 0.1$, so it is hard to extrapolate it past about $M_\infty = 0.6$. Fortunately, it complements the Mach number range of the larger Ref. 9 database quite nicely.

Figure 1 shows one example of the many figures in Ref. 4 for the nonlinear variations of $K_{W(B)}$ and $K_{B(W)}$ with AOA at $M = 1.5$ for an aspect ratio of 0.5 and at $\Phi = 45$ deg. Other Mach number and aspect ratio results are given in Ref. 4. It is clear in examining Fig. 1, and the other figures in Ref. 4, that inclusion of the nonlinearities in the interference factors is essential in accurately developing a semiempirical nonlinear aeroprediction code. Reference 4 does this similarly to Ref. 1, where a mathematical model is developed based on SBT/LT plus deviation of SBT/LT based on data. That is,

$$\begin{aligned} K_{W(B)} &= \left[K_{W(B)}\right]_{\text{SBT}} + \Delta K_{W(B)}(\alpha, M, \text{AR}, \lambda) \\ K_{B(W)} &= \left[K_{B(W)}\right]^{\text{SBT}}_{\text{LT}} + \Delta K_{B(W)}(\alpha, M, \text{AR}, \lambda) \end{aligned} \tag{7}$$

The functions $\Delta K_{W(B)}$ and $\Delta K_{B(W)}$ are defined by 11 tables in Ref. 4.

In examining the nonlinear models for $K_{W(B)}$ and $K_{B(W)}$, it is instructive to try to correlate the mathematical models with the physics of the flow. The wing-body interference factor is somewhat easier to understand than the body-wing interference. The wing-body experimental data show that, at low AOA, slender-body theory gives a reasonable prediction of $K_{W(B)}$ for $\Phi = 45$ deg. As AOA is increased, $K_{W(B)}$ starts decreasing and in some cases decreases below

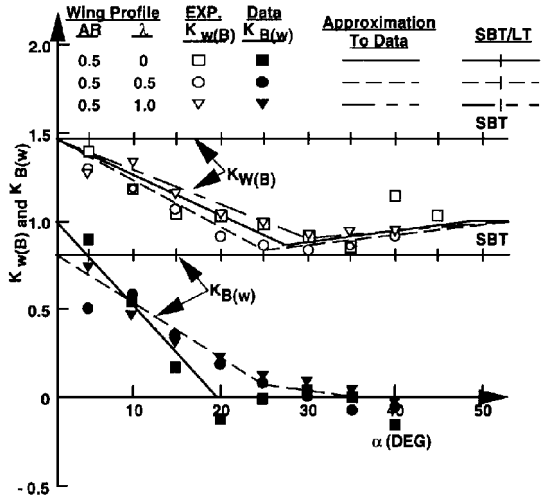

Fig. 1 Wing-body and body-wing interference factors as a function of AOA ($M_\infty = 1.5, r/s = 0.5$).

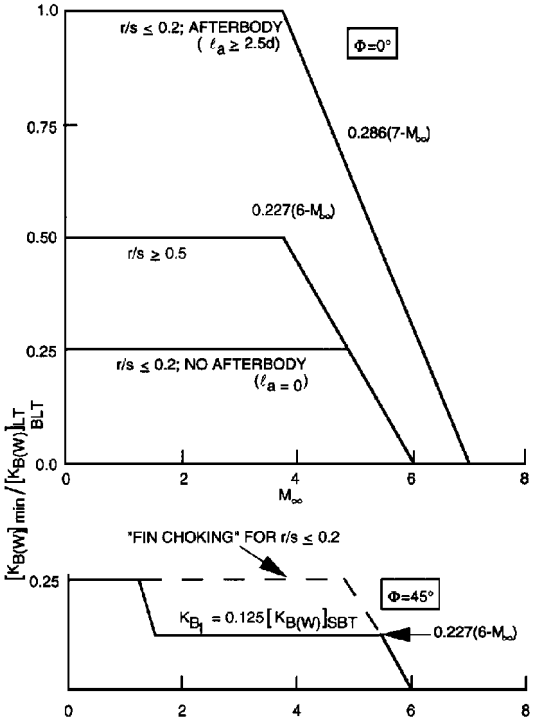

Fig. 2 Minimum value of body-wing interference factor at high AOA.

its wing-alone value. As AOA increases, $K_{W(B)}$ approaches its wing-alone value. As Mach number increases, the positive interference lift on the wing, caused by the presence of the body, is lost faster and faster as AOA increases. That is, the wing-alone solution is recovered much faster at high Mach number, as AOA increases, than at low Mach number. This is believed to be the result of the Newtonian impact mechanism where, at high Mach number, the momentum of the air particle is lost almost entirely upon direct impact on a surface, as opposed to wrapping around the surface and carrying some of the momentum with it, as at low Mach numbers.

The $K_{B(W)}$ model contains body vortex effects, nose- and wing-to-wing shock effects, and the usual added dynamic pressure of the body caused by the presence of the wing. The present direct approach of modeling these effects simultaneously neglects some of the scale effects caused by the position of the wing on the body. The alternative to this approach is to attempt to estimate each of the physical effects analytically, subtract them out of the data, and then add them back in by using the same analytical approach but for a different configuration.[2]

In general, $K_{B(W)}$ decreases as AOA increases. However, a certain amount of lift or force enhancement is gained all the way to $\alpha = 90$ deg for low Mach numbers, as shown in Fig. 2. This phenomenon is assumed to occur all the way to $M = 6.0$ based on extrapolated data from the point where experimental data end.[4]

Additional higher AOA data above $\alpha = 40$ deg are needed for both $K_{W(B)}$ and $K_{B(W)}$ to modify the assumed extrapolations of the models for $K_{W(B)}$ and $K_{B(W)}$ at high AOA. However, until additional data are available, the approximate nonlinear models for $K_{W(B)}$ and $K_{B(W)}$ can be used to estimate aerodynamics for engineering use. This statement will be validated for a limited set of flight conditions in a later section.

Two of the key issues associated with defining the functions $\Delta K_{W(B)}$ and $\Delta K_{B(W)}$ are the variations with r/s and internal shocks. Most of the data available[9] are for $r/s = 0.5$ with only one set of lifting surfaces present. This means that any nonlinearities associated with r/s and internal shocks from forward to rearward lifting surfaces have to be modeled separately or not included. The most critical of these issues appeared to be the minimum value of $K_{B(W)}$ at high AOA.

Figure 2 represents the treatment of $[K_{B(W)}]_{\text{MIN}}$ for both the $\Phi = 0$ deg and the $\Phi = 45$ deg roll positions. This figure was derived based on the Ref. 9 and 10 databases for $r/s = 0.5$ and numerical experiments for other r/s cases. Referring to Fig. 2, note that for $r/s \leq 0.2$, $\Phi = 0$ deg, there is a difference in the minimum value of $K_{B(W)}$ depending on whether there is an afterbody present or not, whereas for $r/s \geq 0.5$ there did not appear to be. It should be remembered that $[K_{B(W)}]_{\text{MIN}}$ is given as a fraction of SBT in Fig. 2. Thus, a value of 1.0 at $r/s = 0.2$ in Fig. 2 gives a value of $[K_{B(W)}]_{\text{MIN}}$ of 0.27, whereas a value of 0.5 for $r/s = 0.5$ gives a value of $[K_{B(W)}]_{\text{MIN}}$ of 0.4. Also note that $[K_{B(W)}]_{\text{MIN}}$ appeared to approach zero at high Mach number. More data or computational fluid dynamics are needed to more precisely define Fig. 2.

Of equal importance in Fig. 2 is the lower curve for $\Phi = 45$ deg. Note that $[K_{B(W)}]_{\text{MIN}}$ is one-half to one-quarter of that for $\Phi = 0$ deg. This lower value of $K_{B(W)}$ appears to be the main reason many missiles have lower normal forces flying at $\Phi = 45$ deg than at $\Phi = 0$ deg, particularly if r/s is fairly high (0.4 or greater). Note also the fact that fin choking is given a separate label for low r/s and $\Phi = 45$ deg.

Fin choking is a phenomenon similar to what occurs when an inlet becomes unstarted or a wind tunnel achieves its maximum rate of flow (an increase in power produces no more mass flow through the inlet). As the body increases in AOA with the fins oriented in the × or cross orientation, the flow between the fins will eventually choke at some AOA and at moderate to large supersonic Mach numbers. When this happens, a strong shock is formed just in front of the fin,[14,15] producing a high-pressure region on the fins and body. This high-pressure region is shifted forward from where it would be if supersonic flow occurred through the fins. Whereas the absolute value of pressure on the body is higher than for the unchoked flow, it occurs over a much smaller region and hence gives only slightly higher body-wing interference lift. Modified Newtonian theory was used in Ref. 4 to define the region where fin choking occurred. It was found that fin choking appeared to occur on wing-dominated (small r/s) configurations at $\Phi = 45$ deg roll but not on body-dominated configurations (large r/s). A fairly thorough discussion of other internal shock interactions was also given in Ref. 4. Suffice it to say that additional work is still needed before internal shock interactions can be completely modeled with a semiempirical code.

Wing-Body and Body-Wing Interference Due to Control Deflection

The same general approach, with slight modifications, to the nonlinear model of Ref. 1 for $\Phi = 0$ deg roll is used for the $\Phi = 45$ deg roll position. In the Ref. 1 method, $k_{W(B)}$ and $k_{B(W)}$ were approximated by

$$k_{W(B)} = C_1(M)\left[k_{W(B)}\right]_{\text{SBT}} + C_2(|\alpha_W|, M) \tag{8}$$

$$k_{B(W)} = \left[k_{B(W)}\right]_{\text{SBT}} \tag{9}$$

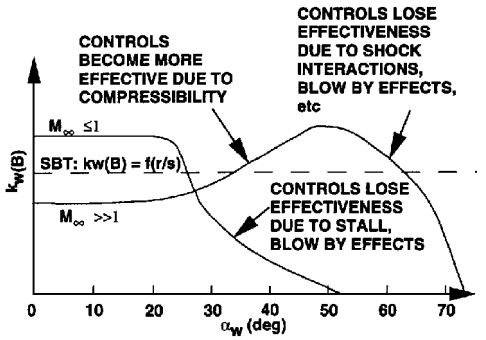

Fig. 3 Qualitative trend of wing-body interference due to control deflection as function of M_∞ and α_W.

The parameters C_1 and C_2 were derived based on numerical experiments of the AP95 compared to data. This numerical definition of C_1 and C_2 was required because many of the fins in the Ref. 9 database were too small to allow accurate estimates of $k_{W(B)}$ as a function of parameters of interest. As a result, total missile load data were used and empirical values of C_1 and C_2 were estimated as a function of combined local AOA of the wing $|\alpha + \delta|$ and Mach number. The tables of C_1 and C_2 for $\Phi = 45$ deg are given in Ref. 4.

In examining the constants and model of Ref. 4, several physical phenomena occur that are modeled in a semiempirical sense by Eqs. (8) and (9). These phenomena are qualitatively shown in Fig. 3. At low Mach number, Fig. 3 indicates the SBT gives a low value of $k_{W(B)}$ for small values of α_W. At a value of α_W of about 25 deg, the controls lose effectiveness as a result of a combination of stall and blow-by effects due to the separation between the wing and body. At an α_W of about 55 deg, the controls have lost all effectiveness. At Mach numbers greater than about 4, the controls initially generate less effectiveness than is generated by SBT for values of α_W up to about 20 or 25 deg. The controls then become more effective because of nonlinear compressibility effects. On the other hand, at an α_W of around 45–50 deg, the controls once again begin to lose effectiveness, presumably because of shock interactions and blow-by effects. For Mach numbers in between subsonic and high supersonic, $k_{W(B)}$ has behavior in between the two extremes illustrated in Fig. 3.

In comparing the nonlinear control deflection models for $\Phi = 0$ and 45 deg roll in Ref. 4, a lot of similarity is seen. The constants for $\Phi = 45$ deg are slightly different from those for $\Phi = 0$ deg and the values of α_W where the nonlinearities begin are somewhat different. However, by and large, Eq. (8) holds for both the $\Phi = 0$ and 45 deg roll cases. In Ref. 1, mostly linear variations of $k_{W(B)}$ with α_W were used. However, these have been improved upon for the $\Phi = 45$ deg case with cubic fits of control deflection data. As such, all nonlinear effects are included in the variations of $k_{W(B)}$ as a function of Mach number and $|\alpha + \delta|$. Also note that $k_{W(B)}$ and $k_{B(W)}$ are multiplied by $\sqrt{2}$ to indicate that all four fins are assumed to be deflected by an equal amount in the $\Phi = 45$ deg roll position.

Reference 4 also derived new semiempirical models for wing-tail interference. This new wing-tail methodology was given in Ref. 15 and thus is not discussed in detail. Suffice it to say that the new methodology was derived based on SBT at low AOA and a nonlinear semiempirical method for higher AOA. However, the comparisons with data in the next section have the new wing-tail interference model included when the configuration has two sets of lifting surfaces present.

Results and Discussion

The new nonlinear aeroprediction methodology for the $\Phi = 45$ deg roll position has been validated against many configurations within and outside the databases upon which the methodology was developed. Reference 4 gives results for seven wing- or tail-body cases and five wing- or canard-body-tail cases. Three cases are chosen here to illustrate the accuracy of the new methodology as well as remaining problems in the state-of-the-art in both experimental testing and semiempirical code development. Two of these cases are given in Ref. 4 in more detail, and the third case has not been shown previously for the $\Phi = 45$ deg roll aerodynamics.

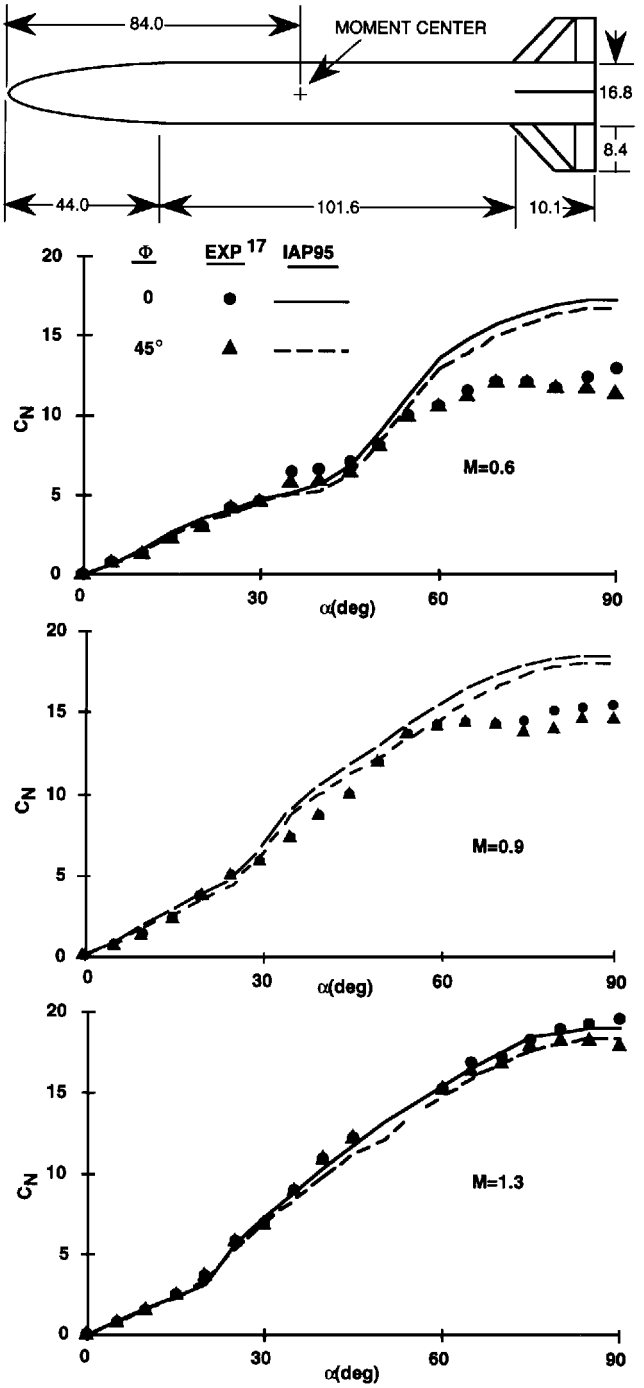

Fig. 4 Normal-force coefficient comparisons of theory and experiment.

The first of these cases is from Ref. 16 and is referred to as the air-slew-demonstrator-vehicle. Data were available at $\Phi = 0$ and 45 deg roll at $M = 0.6-1.3$ and to AOA = 90 deg. Figure 4 shows the configuration schematically and the normal-force coefficient results for $M = 0.6, 0.9$, and 1.3. This case was chosen for several reasons. First, it illustrates the accuracy of the code at $\Phi = 0$ and 45 deg at moderate subsonic Mach numbers to AOA = 90 deg. Second, it illustrates a problem encountered in validating the code at subsonic and transonic Mach numbers based on wind-tunnel data. This problem is wind-tunnel model sting interference.

Reviewing some of the wind-tunnel model support interference literature,[15–21] several conclusions were reached. These were that 1) for low Mach number, the problems of estimating interference effects of a strut or sting mount on the model aerodynamics at high AOA are not known precisely—this is still true today; 2) the

preferable mount between a sting and a strut at high AOA is the sting; 3) the sting tends to give positive interference (C_N too high) and the strut gives negative interference (C_N too low).

The affected region seems to be in the AOA range 30–80 deg. Sting C_N values can be high by as much as 10–15%, and strut C_N values for struts mounted in the midbody region can be low by as much as 25–30%. For these reasons, the improved aeroprediction code 1995 (IAP95) methodology is intentionally designed to underpredict normal force on configurations at subsonic Mach numbers at high AOA, where test data are from a sting mount; therefore, it is also expected that predictions will be higher than those from a strut-mounted model. The under/overprediction problem on C_N at high α appears to go away at Mach numbers slightly greater than one. This reduction in sting interference effects as Mach number increases is suspected to be a result of reduction in the upstream influence of the sting on the body and reduction of the wake effect on the body (strut mount).

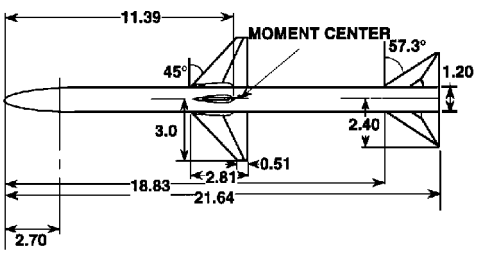

Fig. 5a Air-to-air missile configuration used in validation (from Ref. 22).

Because the Fig. 4 configuration was mounted in the tunnel with a strut, the strut mount is suspected to be the major reason for overprediction of the IAP95 methodology compared to data at $M = 0.6$ and 0.9 and AOA > 50 deg. Although COP predictions are not shown, results are within the $\pm 4\%$ of body-length goal at all AOA and Mach numbers. This implies that any loss of normal force due to the strut is distributed all along the body. Also, if one excludes the AOA > 50 deg comparison at $M = 0.6$ and 0.9, where wind-tunnel measurement errors are in question, the IAP95 is well within the $\pm 10\%$ accuracy goal on normal force as well.

The last two configurations considered in the validation process utilize all the new nonlinear methodology developed for the $\Phi = 0$ and 45 deg roll orientations. The first of these is a version of the Seasparrow missile as shown in Fig. 5a, with wind-tunnel results taken from Ref. 22. This configuration has fairly large wings and tails, with the wings used as the control. Data were taken at Mach numbers of 1.5, 2.0, 2.35, 2.87, 3.95, and 4.63. Figures 5b, 5c, and 5d give comparisons of the IAP95 with the data at $M = 1.5$, 2.87, and 4.63, respectively. Results are shown for control deflections of 10 deg for $M = 1.5$ and 20 deg for $M = 2.87$ and 4.63. Also, all results for the $\Phi = 0$ and 45 deg roll positions are shown. Several comments are in order with respect to the overall comparisons. First, the IAP95 model achieves its goal of predicting an average accuracy of C_A, C_N of $\pm 10\%$ and X_{CP} of $\pm 4\%$ ℓ_B on this configuration at the $\Phi = 0$ and 45 deg roll positions. Second, C_N is predicted equally well at $\Phi = 0$ and 45 deg. However, C_M is predicted better at $\Phi = 45$ deg than at $\Phi = 0$ deg because of the COP shift discussed earlier. No such shift has been applied at $\Phi = 0$ deg. Apparently one is needed, but the physical justification for it is not clear. As seen in the pitching-moment predictions for the $\Phi = 0$ deg roll orientation,

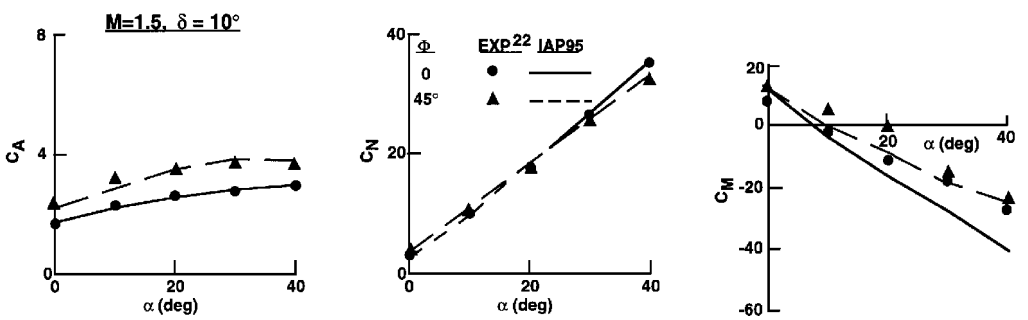

Fig. 5b Axial, normal, and pitching moment coefficient comparison of theory and experiment.

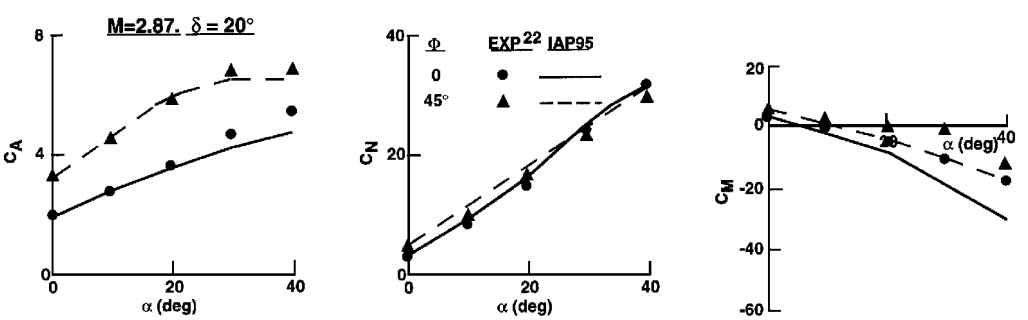

Fig. 5c Axial, normal, and pitching moment coefficient comparison of theory and experiment.

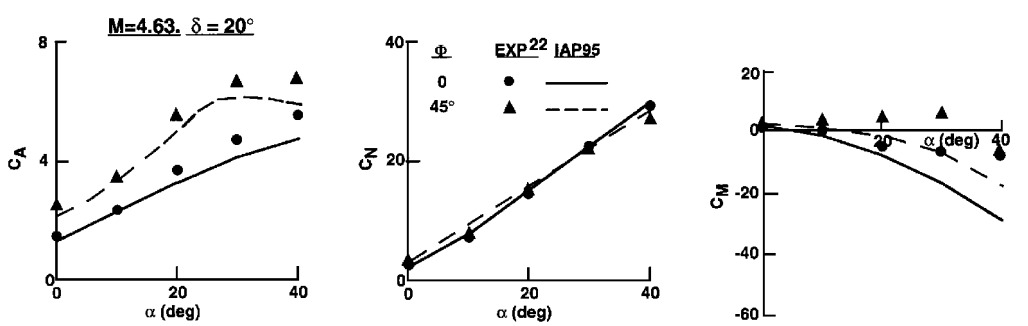

Fig. 5d Axial, normal, and pitching moment coefficient comparison of theory and experiment.

the IAP95 in general is slightly too stable. The third point is that the C_A prediction is slightly better for the $\Phi = 0$ deg roll orientation than the $\Phi = 45$ deg position. Apparently, the factor of $\sqrt{2}$ applied to the fins for the control-deflection component of axial force is quite adequate at low AOA at all Mach numbers, as shown in the figures. However, at high AOA, this factor appears to be too high at the lower supersonic Mach numbers and too low at the higher supersonic Mach numbers. It is suspected that, at the lower supersonic Mach numbers, only the fins in the windward plane should have the full factor of $\sqrt{2}$, whereas those in the leeward plane should have a lower factor. For high supersonic conditions, it is suspected the bow shock and internal shock interactions actually add to the factor of $\sqrt{2}$. An empirical model for the control-deflection component of C_A to account for this physics would improve the C_A comparison, but time did not permit this effort.

The final point to be made is concerning the high Mach number and high AOA conditions in Fig. 5. Note that the pitching moment suddenly loses stability above AOA of 30 deg and $\Phi = 0$ deg roll at $M = 4.63$. The normal force also decreases somewhat. It is believed this may be because of internal shock waves from the bow shock and wing shock intersecting the tail, causing a loss of tail lift and a sudden decrease in stability. No accounting of these internal shocks from a forward-mounted fin to an aft-mounted fin is made in the IAP95. Note that above AOA = 70 deg, although the results are not shown, the IAP95 predictions for pitching moment agree quite well with the data. Apparently the internal shock interactions are important between AOA of about 30–60 deg.

The last configuration chosen for validation of the new methodology against wind-tunnel results is shown in Fig. 6a. The data as well as DATCOM[3] results are taken from Ref. 23. The control is from the canards. The configuration is over 22 calibers long with aspect ratio tails of 0.9 and canards of 1.57. Data were taken for a Mach number of 0.2 but to AOA of 50 deg with control deflections of 0 and ±20 deg. The +20 deg control deflection case is illustrated in Fig. 6b. Both the IAP95 and missile DATCOM results from Ref. 23 are shown along with the data for the $\Phi = 45$ deg roll only. In general, the IAP95 gives very good comparisons with data and appears to exhibit most of the nonlinearities of the data. The IAP95 predictions and missile DATCOM results give reasonably good agreement with data. Reference 1 compared the AP95, missile DATCOM, and data for this same case at $\Phi = 0$ deg roll. The AP95 results were about as good at $\Phi = 0$ deg as at $\Phi = 45$ deg. However, the missile DATCOM gave better results compared to data at $\Phi = 45$ vs 0 deg. It is not known whether this statement holds true in general, however.

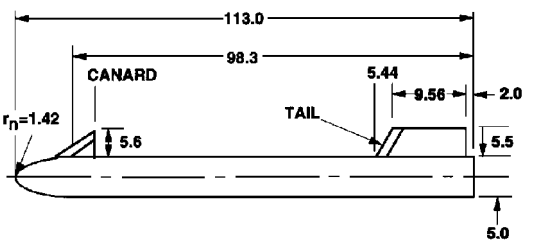

Fig. 6a Canard-controlled missile configuration (all dimensions in inches, full scale).

Summary, Conclusions, and Recommendations

New technology has been developed to allow engineering estimates of aerodynamics of most tactical weapon concepts for the $\Phi = 45$ deg roll position (fins oriented in × or cross-fin arrangement). New technology developed for the $\Phi = 45$ deg roll position and discussed in this paper includes the following:

1) Nonlinear wing-body and body-wing interference factor methodology due to AOA and control deflection.

2) An approximate method to estimate wing-alone shift in COP at $\Phi = 45$ deg and high AOA.

3) An approximate method to account for fin choking at high Mach number and AOA.

This new technology, along with the $\Phi = 0$ deg methodology of Ref. 1, now allows trim aerodynamics to be computed in the two roll-stabilized planes that most of the world's missiles fly. The databases upon which the methodology was based were limited in Mach number to 4.5 and AOA of 40 deg. However, engineering judgment and other data were used to allow calculations to be performed to AOA of 90 deg and Mach numbers up to 20 for axisymmetric solid rocket weapons with up to two sets of lifting surfaces.

Based on the new methodology and computations to date, the following conclusions are made.

1) The two primary reasons missile normal forces are lower at $\Phi = 45$ deg than at $\Phi = 0$ deg are that the minimum value of body carryover lift at high AOA is lower for $\Phi = 45$ deg than $\Phi = 0$ deg. The larger the value of r/s, the more difference between these minimum values. If the configuration has two sets of lifting surfaces, the wing-tail interference is higher for AOA > 20 deg for the $\Phi = 45$ deg plane than for the $\Phi = 0$ deg plane, also contributing to a lower normal force for $\Phi = 45$ deg and a less stable configuration.

2) At high AOA, $K_{W(B)}$ approaches 1.0 for most Mach numbers; $K_{B(W)}$ approaches some minimum value that is a function of r/s and Mach number; and $k_{W(B)}$ and $k_{B(W)}$ are nonlinear in total local AOA on the wing and are functions of Mach number and total AOA on the wing.

3) Fin choking appears to be more of a problem on larger fin (small r/s) configurations at $\Phi = 45$ deg than on smaller fin cases (large r/s).

4) For Mach numbers less than one and AOA > 30 deg, it is not clear what the correct values of experimental normal force are for a given configuration based on wind-tunnel results available in the literature.

5) Internal shock interactions between forward-mounted and aft-mounted fins become increasingly important as both AOA and Mach number increase. The current methodology does not account for these effects.

6) In general, ± 10% average accuracy has been maintained for both normal- and axial-force coefficients and ± 4% of body length for COP in the $\Phi = 45$ deg roll position. Exceptions to this are at subsonic Mach number and high AOA where data accuracy is in question and at high Mach number and high AOA for configurations that have two sets of lifting surfaces where internal shock interactions may be a problem.

7) The current overall approach of using linear theory, slender-body theory, or second-order theory for low AOA aerodynamics and estimating the nonlinear aerodynamic terms individually and

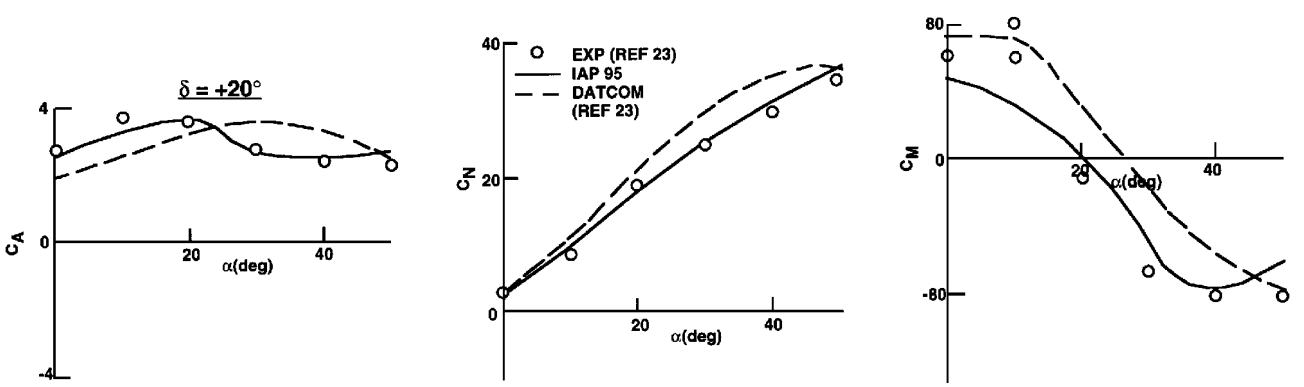

Fig. 6b Axial, normal, and pitching moment coefficient comparisons of theory and experiment ($M = 0.2$ and $\Phi = 45$ deg).

directly from wind-tunnel databases appears to be the key to the average accuracy levels mentioned earlier.

Based on this and previous research,[1,6] the following recommendations are made for additional work.

1) Additional wind-tunnel measurements or computational fluid dynamics cases need to be made to help define nonlinearities of the interference effects as a function of r/s.

2) A method is needed to accurately correct wind-tunnel data at subsonic Mach number and high AOA for sting- or strut-mounting effects.

3) An engineering method is needed to estimate internal shock interaction effects for high AOA and Mach number.

4) Any future wind-tunnel test for measuring component aerodynamics should be done with lifting surfaces large enough to separate out body and wing lift accurately, with wings mounted in the middle of the body and, preferably, with simultaneous measurements of body forces in conjunction with the wing and wing forces in conjunction with the body. This would allow more accurate determination of the interference terms directly, without subtraction of two large numbers to obtain a small term.

Acknowledgments

The work described in this paper was supported through the U.S. Office of Naval Research (Dave Siegel) by the following programs: the Air Launched Weapons Program managed at the Naval Air Warfare Center, China Lake, California, by Tom Loftus and Craig Porter, and the Surface Weapons Systems Technology Program managed at the U.S. Naval Surface Warfare Center, Dahlgren Division (NSWCDD), by Robin Staton and Gil Graff. Also, some support was provided in fiscal year 1994 by the Army Missile Command at Huntsville, Alabama, under Dave Washington and in fiscal year 1995 by the Marine Corps Weaponry Technology Program managed at NSWCDD by Bob Stiegler. The authors express appreciation for support received in this work. Appreciation is also given to Tom Hymer, who provided some data used in the validation process.

References

[1]Moore, F. G., McInville, R. M., and Hymer, J. C., "The 1995 Version of the NSWC Aeroprediction Code: Part I—Summary of New Theoretical Methodology," U.S. Naval Surface Warfare Center, NSWCDD/TR-94/379, Dahlgren, VA, Feb. 1995.

[2]Nielsen, J. N., Hemsch, M. J., and Smith, C. A., "A Preliminary Method for Calculating the Aerodynamic Characteristics of Cruciform Missiles to High Angles of Attack Including Effects of Roll Angle and Control Deflections," U.S. Office of Naval Research, ONR-CR215-226-4F, Arlington, VA, Nov. 1977.

[3]Vukelich, S. R., Stoy, S. L., Burns, K. A., Castillo, J. A., and Moore, M. E., "Missile DATCOM Volume I—Final Report," AFWAL-TR-86-3091, Wright–Patterson AFB, OH, Dec. 1988.

[4]Moore, F. G., and McInville, R. M., "Extension of the NSWCDD Aeroprediction Code to the Roll Position of 45 Degrees," U.S. Naval Surface Warfare Center, NSWCDD/TR-95/160, Dahlgren, VA, Dec. 1995.

[5]Walters, R. W., Slack, D. C., Cinnella, P., Applebaum, M. P., and Frost, C. A., "Users Guide to GASP," Dept. of Aerospace and Ocean Engineering, Virginia Polytechnic Inst. and State Univ., Blacksburg, VA, Nov. 1990.

[6]Moore, F. G., Hymer, T., and Devan, L., "New Methods for Predicting Nonlinear Lift, Center of Pressure, and Pitching Moment on Missile Configurations," U.S. Naval Surface Warfare Center, NSWCDD/TR-92/217, Dahlgren, VA, July 1992.

[7]Stallings, R. L., Jr., and Lamb, M., "Wing-Alone Aerodynamic Characteristics for High Angles of Attack at Supersonic Speeds," NASA 1889, July 1981.

[8]Baker, W. B., Jr., "Static Aerodynamic Characteristics of a Series of Generalized Slender Bodies With and Without Fins at Mach Numbers from 0.6 to 3.0 and Angles of Attack from 0 to 180°," Arnold Engineering Development Center, AEDC-TR-75-124, Vols. 1 and 2, Tullahoma, TN, May 1976.

[9]Allen, J. M., Tri-Service Missile Data Base, NASA Langley Research Center, transmitted to U.S. Naval Surface Warfare Center, Nov. 1991 (formal documentation in process).

[10]Meyer, J., "Effects of the Roll Angle on Cruciform Wing-Body Configurations at High Incidences," *Journal of Spacecraft and Rockets*, Vol. 31, No. 1, 1994, pp. 113–122.

[11]Ashley, H., and Martin, M., *Aerodynamics of Wings and Bodies*, 1st ed., Addison–Wesley, Reading, MA, 1965, pp. 99–171.

[12]Nielsen, J. N., *Missile Aerodynamics*, 2nd ed., Nielsen Engineering and Research, Mountain View, CA, 1988, pp. 34–201.

[13]Allen, J. H., and Perkins, E. W., "Characteristics of Flow over Inclined Bodies of Revolution," NACA RM A 50L07, March 1951.

[14]Stallings, R. L., Jr., Lamb, M., and Watson, C. B., "Effect of Reynolds Number on Stability Characteristics of a Cruciform Wing-Body at Supersonic Speeds," NASA TP 1683, July 1980.

[15]Agnone, A. M., Zakkay, V., Tory, E., and Stallings, R., "Aerodynamics of Slender Finned Bodies at Large Angles of Attack," AIAA Paper 77-0666, June 1977.

[16]Whoric, J. M., and Washington, E. S., "Aerodynamic Characteristics of the Air Slew Demonstrator Models at Mach Numbers 0.6 to 1.3," Arnold Engineering Development Center, AEDC TR-76-92, Tullahoma, TN, Aug. 1976.

[17]Moore, F. G., and McInville, R. M., "A New Semiempirical Model for Wing-Tail Interference," AIAA Paper 96-3393, July 1996.

[18]Dietz, J., and Altstatt, M. C., "Experimental Investigation of Support Interference on an Ogive Cylinder at High Incidence," *Journal of Spacecraft and Rockets*, Vol. 16, No. 2, 1979, pp. 67, 68.

[19]Canning, T. N., and Nielsen, J. N., "Experimental Study of the Interference of Supports on the Aerodynamic Loads on an Ogive Cylinder at High Angles of Attack," AIAA Paper 81-0007, Jan. 1981.

[20]Nelson, R. C., and Mouch, T. N., "Cylinder/Splitter-Plate Data Illustrating High α Support Interference," *Journal of Spacecraft and Rockets*, Vol. 16, No. 2, 1979, pp. 126, 127.

[21]Ericsson, L. E., and Reding, J. P., "Review of Support Interference in Dynamic Tests," *AIAA Journal*, Vol. 21, No. 12, 1983, pp. 1652–1662.

[22]Monta, W. J., "Supersonic Aerodynamic Characteristics of a Sparrow III Type Missile Model with Wing Controls and Comparison with Existing Tail Control Results," NASA TP 1078, Nov. 1977.

[23]Smith, E. H., Hebbar, S. K., and Platzer, M., "Aerodynamic Characteristics of a Canard-Controlled Missile at High Angles of Attack," AIAA Paper 93-0763, Jan. 1993.

R. M. Cummings
Associate Editor